A POSSIBLE APPLICATION OF THREE-DIMENSIONAL MODELLING FOR DEEP LAKES HYDROTHERMAL STUDIES

G. Dinelli

A. Tozzi

September 1978 WP-78-33

2361
Laxenburg
Austria

International Institute for Applied Systems Analysis

A Possible Application of Three-Dimensional Modelling For Deep Lakes Hydrothermal Studies

G. Dinelli and A. Tozzi

Introduction

Several phenomena relating to the ecology of deep lakes and reservoirs depend on the hydrothermal processes and circulation patterns in the specific site which are influenced by seasonal natural events as well as by urban and industrial pollutants sources.

Moreover the planning, design and control of cooling systems and/or pollutant effluents require predictive mathematical models in order to simulate the local and mesoscale effects of pollutants under normal and extreme environmental conditions and for the adoption of the most economical design parameters and control strategies.

In this respect a multi-layer three-dimensional model (TRIMDI) has been recently investigated at ENEL for use in ecological studies under complex geographic situations or when multiple releases result in interaction with the boundaries of the receiving water body.

Basic Assumptions and Boundary Conditions

The TRIMDI model is based on the numerical solution of the Navier-Stokes equations describing a three-dimensional time dependent stratified flow in presence of heat and mass transfer. A schematic view of a typical system to be studied is shown in Fig. 1 together with the computational grid used.

The main assumption upon which the code has been developed is that the vertical distribution of pressure is hydrostatic which implies that any source of momentum in the system such as intakes and discharges must have horizontal components only.

The system under study is subdivided into several horizontal layers coupled by the vertical transfer of mass, momentum and energy; in addition the depth of the surface layer is variable to account for variable wind and atmospheric pressure induced effects.

Inside each layer the basic three-dimensional equations are integrated in the vertical direction; the sub-sets of equations thus generated for each horizontal layer are coupled by the terms describing the shear stress and heat transfer between layers and the vertical convection. The dispersion of pollutants is described by adding the relative equation of conservation. Finally the density variations with temperature (pollutant concentration) is taken into account following the Boussinesq approximation.

The model governing equations are shown in Table 1. The source terms Φ^u, Φ^v and Φ^T account for minor effects due to the spatial derivatives of the diffusion coefficients and of the surface layer depth. These are negligible unless an abrupt change in physical conditions such as a storm occurs. If required, the source terms may include Coriolis effects. The horizontal shear stress τ_{ij} and the heat transfer between layers are evaluated through empirical correlations for stratified flows.

Initial conditions are introduced for all the variables as well as for ambient conditions such as wind speed and direction, currents, atmospheric pressure.

Boundary conditions are:

- surface wind and atmospheric pressure;
- flow velocities at intakes and discharges;
- temperatures (and pollutant concentrations) at discharges;
- adiabatic no-slip and no-normal velocity conditions at solid boundaries;
- assigned values at open boundaries for temperature (and concentrations) or their first derivatives normal to the boundaries;

- the surface water-air heat transfer (q^s) and the wind shear stress (τ_{ij}) are evaluated as a function of the surface thermal alteration and wind velocity using algebraic expressions.

  The introduction of the boundary conditions is discussed together with the description of the system topology.

Finite Difference Scheme and Computational Procedure

The governing equations are first integrated on a horizontal non-uniform shifted grid, shown in Fig. 1, and then discretized employing forward differences in time and central differences in space except for the convection terms for which donor cell (upwind) difference are used. The finite difference set of equations is shown in Table 2.

The finite difference equations have been written with reference to the values of the variables at point (i, j) and its adjacent points. The coefficients A,...,F are obviously a function of the dependent variables. It is worth noting that for the surface layer the dependent variables are the products ($u_n h_n$), ($v_n h_n$), ($T_n h_n$) instead of u_n, v_n, T_n.

With reference to Table 2, the right hand side of the equations can be evaluated at n-time level (explicit solution); at (n + 1)-time level (implicit solution) or each term can be split into two parts one of which is evaluated at time n and the other at time n + 1. The main advantage of the explicit scheme consists in its simplicity associated with small computer memory storage since the left hand side of equations is known at each time step. However the time step value is limited by stability criteria.

The implicit scheme needs higher memory storage since the nodal values of the coefficients A,...,F must be stored during a time cycle; furthermore the variables are evaluated by inverting pentadiagonal matrices for each layer. For each time step several iterations may be needed to account for non-linear effects and the coupling between layers; however, larger time steps

may be adopted. An advantage of the implicit scheme is that it can be adjusted to give directly the steady state solutions.

Given the initial conditions at time t_o for all the variables, the computation starts with assumed values of variables u^*, v^*, w^*, T^*, h_n^* at time $t_o + \Delta t$.

First the pressure field distribution is determined from the state and hydrostatic equations, then the x-Momentum and y-Momentum equations are solved with standard algorithm for penta-diagonal matrices to obtain the spatial distribution of the horizontal components of the velocity. At each time step the coefficients A,...,F are evaluated from updated values of the variables.

Then the distribution of the vertical component of the velocity is computed by solving the continuity equation for the inner layers starting from the bottom and finally the continuity equation is solved for the surface layer giving the time derivatives of the surface height and therefore the surface depth h_n at time $t_o + \Delta t$.

The computed value of h_n is compared with the initial assumed h_n^* and the cycle is repeated until the convergence is reached.

The next step consists in solving the energy equation to obtain the temperature distribution at time $t_o + \Delta t$. The new spatial distribution of temperature will modify the density and pressure distributions, thus requiring additional iterations in the velocity computation cycle. The convergence check for inner iterations is made on the maximum deviation of successive temperature values. The time is then increased and the procedure repeated until the final state is reached.

The TRIMDI Code makes use of a SIMPLE-like algorithm to correct the surface height each iteration cycle for the velocity field [1]. The algorithm consists in assuming the following correction terms:

$$(h_n U_n)' \sim \frac{\delta (hnhn)'}{\delta x} \quad , \quad (h_n V_n)' \sim \frac{\delta (hnhn)'}{\delta y} \quad , \quad U_k' \sim \frac{\delta hn'}{\delta x} \quad , \quad V_k' \sim \frac{\delta hn'}{\delta y}$$

$$k = 1, 2, \ldots, n-1 \quad ,$$

which are then introduced into the continuity equation for each layer.

By adding these equations one obtains a Poisson equation in the unknown h_n which is solved with the same algorithm employed to solve the momentum and energy equation systems.

System Topology Description

To ease the input-output operations, namely the definition of the geometry of the system, a special sub-programme (TOPY) has been implemented which makes use of a user-oriented language. The main activities of the TOPY sub-programme are:

- the geometry is given through a limited set of parameters describing mainly the irregularities in the boundary region;
- the dimensions of the matrices used in the main programme are defined according to the problem requirements;
- the boundary conditions for the solution of the partial differential equations are set automatically from the input data;
- a check is performed on the geometrical compatibility of the input data;
- an optional output of previous activities consists of a full description of the geometry and boundary conditions of the system under study which are printed before actual computation starts.

The TOPY sub-programme allows an easy description of complex geometries including, for instance, indented coasts, islands, intake and discharge channels, floating platforms, etc.

The topology of the system under study is described through the following input data:

- first the number of strings along the y-direction and the number of cells within each string which are identical are defined for each layer;

- then each cell is characterized as fluid, solid or fluid-solid boundary;

layers with equal topology need not be redefined.

The TOPY sub-programme assigns automatically the boundary condition i.e., no-slip and adiabatic wall at solid boundaries; specific values for the velocity and temperature or for the velocity derivatives are also assigned as input data.

When requested, the topology of each layer is printed by assigning an 0-flag to solid cells, an 1-flag to fluid cells and a 2-flag to open boundaries such as discharge channels.

The TOPY sub-programme has so far been tested with reference to the Bay of Vado Ligure shown in Fig. 2. The adopted computational grid is given in Fig. 3. The bay was subdivided into six vertical layers whose topology is given in Figs. 4, 5, and 6 as they were printed out by the TOPY sub-programme. As a reference the assigned boundary conditions for the velocity and temperature field as well as the location of any source of mass, momentum and pollutants are also printed.

Conclusions

Several three-dimensional models have been presented in recent years for the study of the dispersion of pollutants in large water bodies [2], [3].

To reduce computer running costs in solving the basic Navier-Stokes equations several approximations are introduced, the most important of which is the hydrostatic approximation for the vertical distribution of pressure; moreover, the water body under study is subdivided into layers where the flow is considered to be almost two-dimensional and sometimes also the rigid-lid approximation is adopted [4], [5].

The three-dimensional models have been tested so far with reference to relatively simple situations and few comparisons with field data have been attempted. It seems that the computer running costs should be drastically reduced before such models

can be employed for wide engineering and planning applications. In fact the assessment of the environmental impact of different alternatives under normal and extreme ambient conditions would require practicable predictive models. Thus a practical approach may consist in using mathematical models of different complexity in accordance to the specific situation under study.

The validation of the multi-layer TRIMDI model described in the paper will be carried on by comparison with field data collected during the last few years on riverine and coastal effluents using airborne infra-red surveys associated with in situ measurements at several water depths [6]. Furthermore, this comparison should allow also the definition of a suitable turbulence model to represent the mass and heat dispersion mechanisms adequately. The sensitivity of the model to boundary conditions and input data will also be verified.

References

[1] Patankar, S.V., and D.B. Spalding, *A Calculation Procedure for Heat, Mass and Momentum Transfer in Three-Dimensional Parabolic Flows*, BL/TN/A/45, Mech. Eng. Dept. Report, Imperial College, London, 1971.

[2] Policastro, A.J., and W.E. Dunn, *Numerical Modelling of Surface Thermal Plumes*, presented at the Int. Heat and Mass Transfer Centre Seminar, Dubrovnik, 1976.

[3] Cheng, R.T., T.M. Powell, and T.M. Dillon, Numerical Models of Wind-Driven Circulation in Lakes, *Appl. Math. Modelling*, 1, 12, 1976.

[4] Paul, J.F., and W.J. Lick, *A Numerical Model for a Three-Dimensional Variable-Density Jet*, FTAS/TR/73-92, Case Inst. of Technology Report, Cleveland, Ohio, 1974.

[5] Sengupta, S., *A Three-Dimensional Numerical Model for Closed Basins*, presented at the ASME Winter Annual Meeting, 76-WA/HT-21, New York, 1976.

[6] Dinelli, G., and M. Maini, *Remote Sensing of Thermal Alterations and Circulation Patterns of Riverine and Coastal Effluents*, presented at the IFAC Symposium on Environmental Systems Planning, Design and Control, Kyoto, 1977.

Table 1. TRIMDI model governing equations.

Conservation of Mass

surface layer

$$\frac{\delta h_n}{\delta t} + \frac{\delta(u_n h_n)}{\delta x} + \frac{\delta(v_n h_n)}{\delta y} - (w)_{Hn} = 0$$

inner layers

$$h_k \left(\frac{\delta u_k}{\delta x} + \frac{\delta v_h}{\delta y}\right) + (w)_{H_{k+1}} - (w)_{H_k} = 0 \qquad (k = 1,2,\ldots,n-1)$$

Conservation of x-Momentum

surface layer

$$\frac{\delta(u_n h_n)}{\delta t} + \frac{\delta(u_n^2 h_n)}{\delta x} + \frac{\delta(u_n v_n h_n)}{\delta y} - (uw)_{H_n} =$$

$$- \frac{1}{\rho_0} \frac{\delta(P_n h_n)}{\delta x} + \frac{\delta}{\delta x}\left(\nu_n^t \frac{\delta(u_n h_n)}{\delta x}\right) + \frac{\delta}{\delta y}\left(\nu_n^t \frac{\delta(u_n h_n)}{\delta y}\right) + \frac{1}{\rho_0}\left((\tau_{xz}^s)_n - (\tau_{xz})_{H_n}\right) + \Phi_n^u$$

inner layers

$$\frac{\delta u_k}{\delta t} + \frac{\delta u_k^2}{\delta x} + \frac{\delta u_k v_k}{\delta \gamma} + \frac{1}{h_k}\left((uw)_{H_{k\,1}} - (uw)_{H_k}\right) = - \frac{1}{\rho_0} \frac{\delta P_k}{\delta x} + \frac{\delta}{\delta x}\left(\nu_k^t \frac{\delta u_k}{\delta x}\right)$$

$$+ \frac{\delta}{\delta y}\left(\nu_k^t \frac{\delta u_k}{\delta y}\right) + \frac{1}{\rho_0 h_k}\left((\tau_{xz})_{H_{k+1}} - (\tau_{xz})H_k\right) + \Phi_k^u \qquad (k = 1,2,\ldots,n-1)$$

Conservation of y-Momentum

surface layer

$$\frac{\delta(v_n h_n)}{\delta t} + \frac{\delta(u_n v_n h_n)}{\delta x} + \frac{\delta(v_n^2 h_n)}{\delta y} - (vw)_{H_n} =$$

Table 1. (cont'd)

$$-\frac{1}{\rho_0}\frac{\delta(P_n h_n)}{\delta y}+\frac{\delta}{\delta x}\left(\nu_n^t\frac{\delta(v_n h_n)}{\delta x}\right)+\frac{\delta}{\delta y}\left(\nu_n^t\frac{\delta(v_n h_n)}{\delta y}\right)+\frac{1}{\rho_0}\left((\tau_{yz}^s)-(\tau_{yz})_{H_n}\right)+\Phi_n^v$$

inner layers

$$\frac{\delta v_k}{\delta t}+\frac{\delta(u_k v_k)}{\delta x}+\frac{\delta(v_k^2)}{\delta y}+\frac{1}{h_k}\left((vw)_{H_{k+1}}-(vw)_{H_k}\right)=$$

$$\frac{1}{\rho_0}\frac{\delta P_k}{\delta y}+\frac{\delta}{\delta x}\left(\nu_k^t\frac{\delta v_k}{\delta x}\right)+\frac{\delta}{\delta y}\left(\nu_k^t\frac{\delta v_k}{\delta y}\right)+\frac{1}{\rho_0 h_k}\left((\tau_{yz})_{H_{k+1}}-(\tau_{yz})_{H_k}\right)+\Phi_k^v$$

$(k = 1,2,\ldots,n-1)$

Conservation of z-Momentum (vertical)

surface layer

$$P_n = P_{at}+\frac{1}{2}h_n\rho_n g_n$$

inner layers

$$P_k = P_{at}+\frac{1}{2}h_k\rho_k g+\sum_{o\,i}^{n-1-i} h_{n-i}\rho_{n-i}g \qquad (k = 1,2,\ldots,n-1)$$

Conservation of Energy

surface layer

$$\frac{\delta(T_n h_n)}{\delta t}+\frac{\delta(u_n T_n h_n)}{\delta x}+\frac{\delta(v_n T_n h_n)}{\delta y}-(wT)_{H_n}=$$

$$\frac{\delta}{\delta x}\left(\alpha_n^t\frac{\delta(T_n h_n)}{\delta x}\right)+\frac{\delta}{\delta y}\left(\alpha_n^t\frac{\delta(T_n h_n)}{\delta y}\right)+q^s-q_{H_n}+\Phi_n^T$$

Table 1. (cont'd)

inner layers

$$\frac{\delta T_k}{\delta t} + \frac{\delta(u_k T_k)}{\delta x} + \frac{\delta(v_k T_k)}{\delta y} + \frac{1}{h_k}\left((wT)_{H_{k+1}} - (wT)_{H_k}\right) =$$

$$\frac{\delta}{\delta x}\left(\alpha_k^t \frac{\delta T_k}{\delta x}\right) + \frac{\delta}{\delta y}\left(\alpha_k^t \frac{\delta T_k}{\delta y}\right) + \frac{1}{h_k}\left(q_{H_{k+1}} - q_{H_k}\right) \qquad (k = 1,2,\ldots,n-1)$$

Table 2. TRIMDI model finite difference equations.

Conservation of Mass

surface layer

$$h_n^{n+1}(i,j) + \Delta t \left(\frac{p_u^{n+1}(i+1,j) - p_u^{n+1}(i,j)}{\Delta x_i} - \frac{p_v^{n+1}(i,j+1) - p_v^{n+1}(i,j)}{\Delta y_j} \right)$$

$$- \Delta t w^{n+1}(i,j,n) = h_n^n(i,j)$$

inner layers

$$\frac{u_k^{n+1}(i+1,j) - u_k^{n+1}(i,j)}{\Delta x_i} + \frac{v_k^{n+1}(i,j+1) - v_k^{n+1}(i,j)}{\Delta y_i}$$

$$+ \frac{w^{n+1}(i,j,k+1) - w^{n+1}(i,j,K)}{h_k} = 0 \qquad (k = 1,2,\ldots,n-1)$$

Conservation of x-Momentum

surface layer

$$\frac{p_u^{n+1}(i,j) - p_u^n(i,j)}{\Delta t} = A_{(p_u)} p_u(i,j) + B_{(p_u)} p_u(i+1,j) + C_{(p_u)} p_u(i-1,j) +$$

$$D_{(p_u)} p_u(i,j+1) + E_{(p_u)} p_u(i,j-1) + F_{(p_u)}$$

inner layers

$$\frac{u_k^{n+1}(i,j) - u_k^n(i,j)}{\Delta t} = A_{(u_k)} u_k(i,j) + B_{(u_k)} u_k(i+1,j) + C_{(u_k)} u_k(i-1,j)$$

$$+ D_{(u_k)} u_k(i,j+1) + E_{(u_k)} u_k(i,j-1) + F_{(u_k)} \qquad (k = 1,2,\ldots,n-1)$$

Table 2. (cont'd)

Conservation of y-Momentum

surface layer

$$\frac{p_v^{n+1}(i,j) - p_v^n(i,j)}{\Delta t} = A_{(p_v)}p_v(i,j) + B_{(p_v)}p_v(i+1,j) + C_{(p_v)}p_v(i-1,j)$$

$$+ D_{(p_v)}p_v(i,j+1) + E_{(p_v)}p_v(i,j-1) + F_{(p_v)}$$

inner layers

$$\frac{v_k^{n+1}(i,j) - v_k^n(i,j)}{\Delta t} = A_{(v_k)}v_k(i,j) + B_{(v_k)}v_k(i+1,j) + C_{(v_k)}v_k(i-1,j)$$

$$+ D_{(v_k)}v_k(i,j+1) + E_{(v_k)}v_k(i,j-1) + F_{(v_k)} \qquad (k = 1,2,\ldots,n-1)$$

Conservation of z-Momentum (Hydrostatic equations)

surface layer

$$p_n^{n+1} - \frac{1}{2}h_n^{n+1}(i,j)\rho_n^{n+1}(i,j)g - p_{at}^n(i,j) = 0$$

inner layers

$$p_k^{n+1}(i,j) - \sum_{o\ r}^{n-k-1} h_{n-r}^{n+1}\rho_{n-r}^{n+1}(i,j)g - \frac{1}{2}h_k\rho_k^{n+1}(i,j)g - P_{at}^{n+1}(i,j) = 0$$

$$(k = 1,2,\ldots,n-1)$$

Conservation of Energy

surface layer

$$\frac{p_T^{n+1}(i,j) - p_T^n(i,j)}{\Delta t} = A_{(p_T)}p_T(i,j) + B_{(p_T)}p_T(i+1,j) + C_{(p_T)}p_T(i-1,j)$$

Table 2. (cont'd)

$$+ D_{(p_T)} p_T(i,j+1) + E_{(p_T)} p_T(i,j-1) + F_{(p_T)}$$

inner layers

$$\frac{T_k^{n+1}(i,j) - T_k^n(i,j)}{\Delta t} = A_{(T_k)} T_k(i,j) - B_{(T_k)} T_k(i+1,j) + C_{(T_k)} T_k(i-1,j)$$

$$+ D_{(T_k)} T_k(i,j+1) + E_{(T_k)} T_k(i,j-1) + F_{(T_k)} \qquad (k = 1,2,\ldots,n-1)$$

$$p_u = h_n u_n \quad , \qquad p_v = h_n v_n \quad , \qquad p_T = h_n T_n \quad .$$

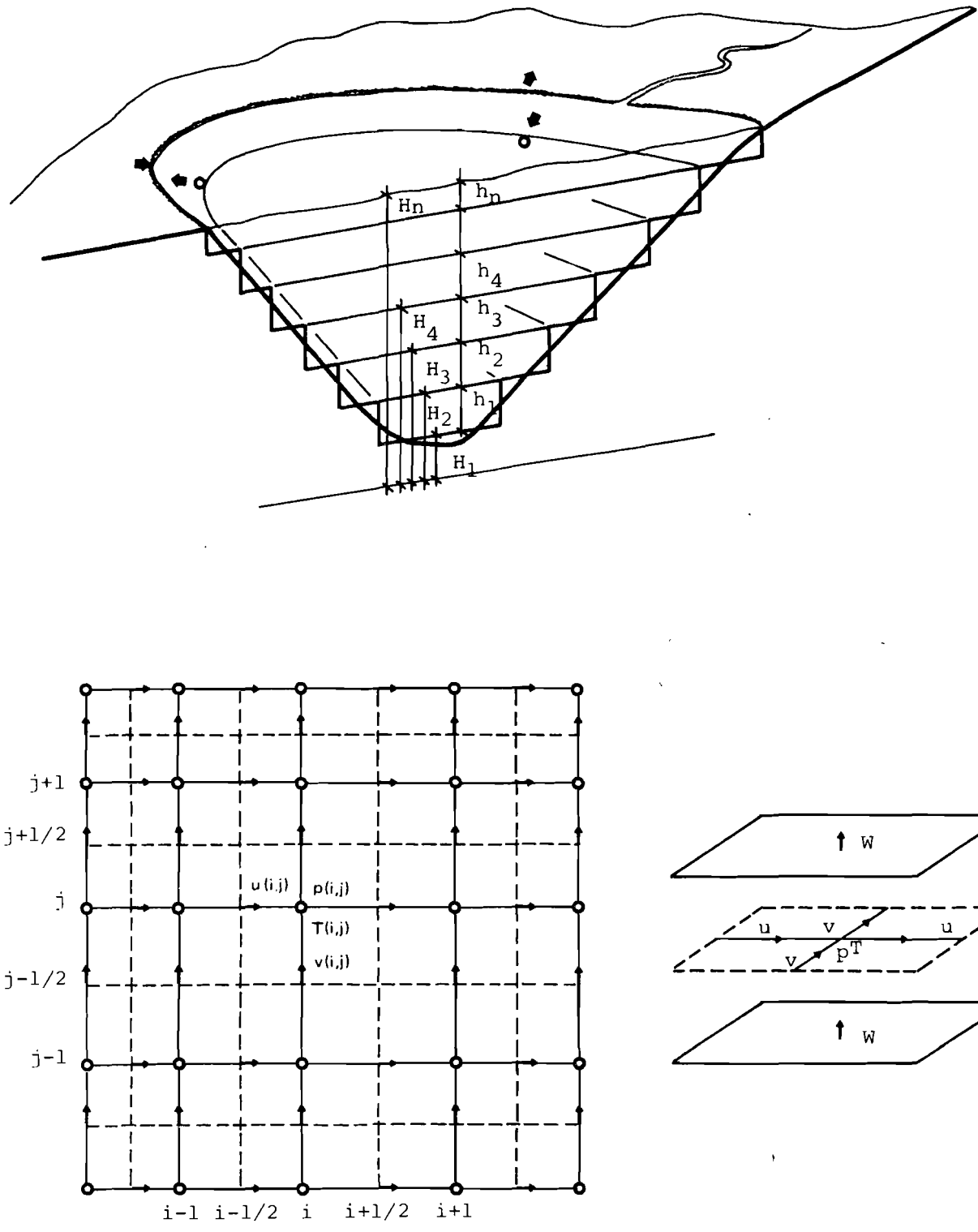

Figure 1. TRIMDI model multi-layer representation and computational grid.

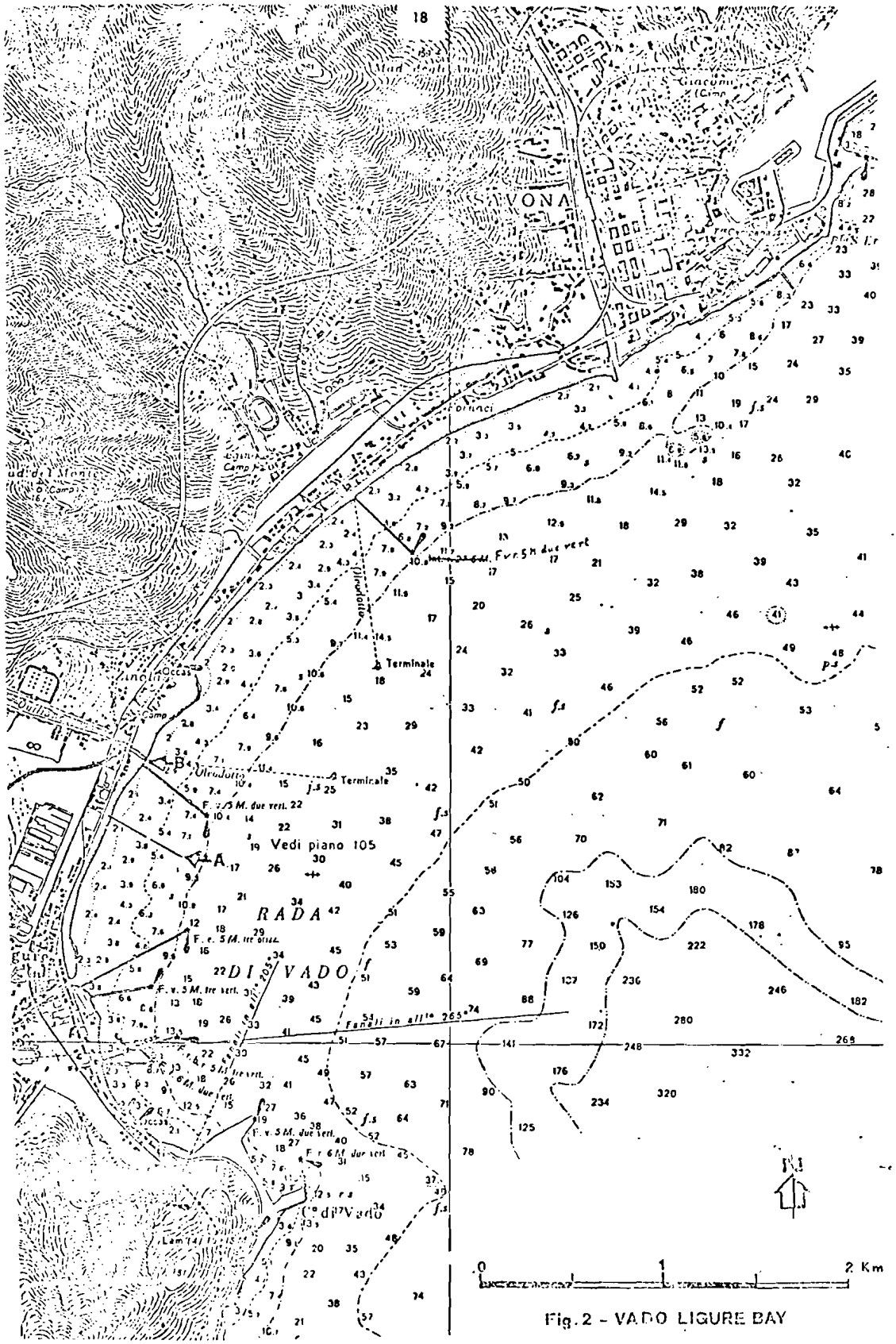

Figure 2. Vado Ligure Bay

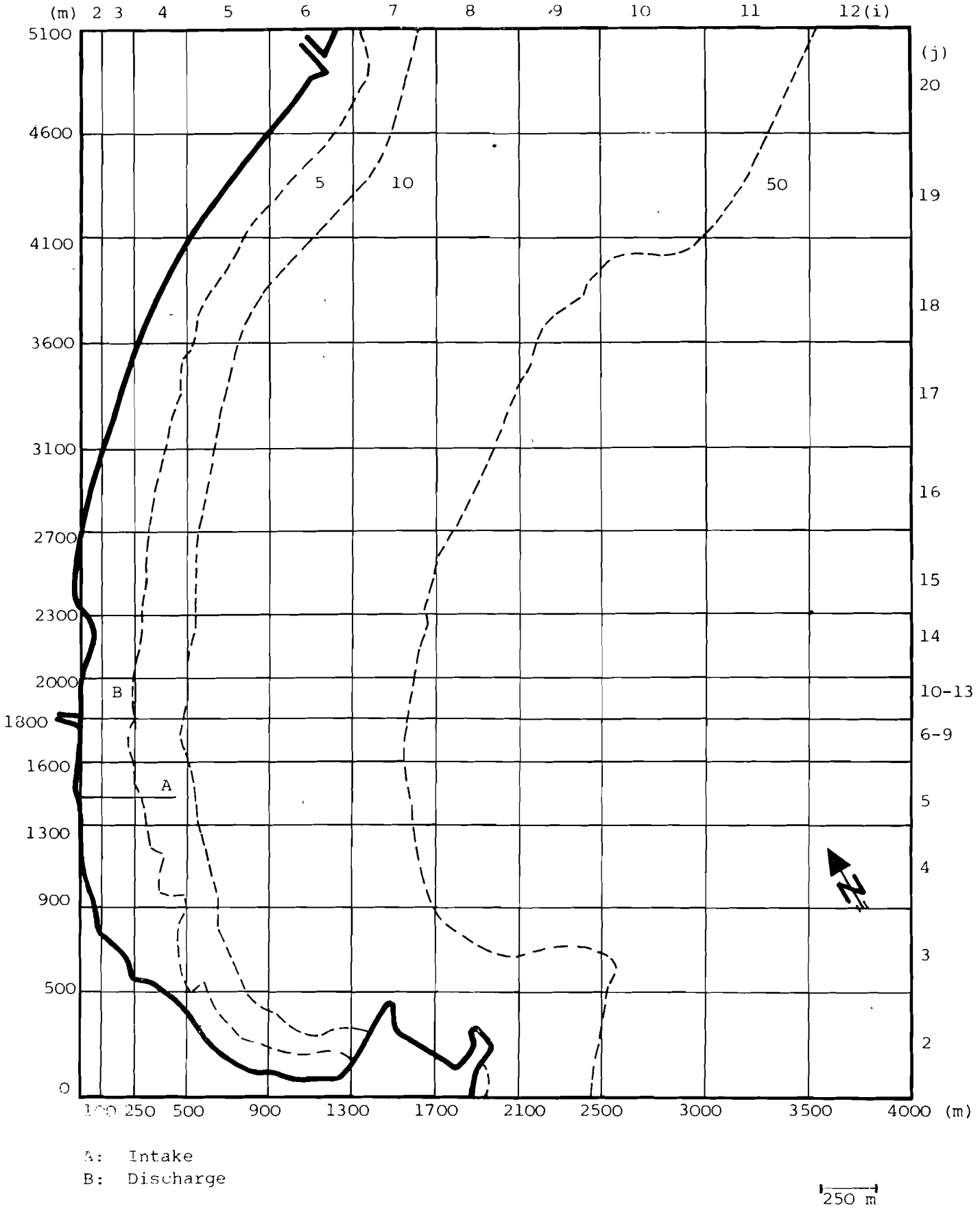

Figure 3. Horizontal computational grid for the Vado Ligure Bay.

STRATO 1

0 CELLE SOLIDE
1 CELLE DI FLUIDO
2 CELLE DI CONTORNO APERTO

	1	2	3	4	5	6	7	8	9	10	11	12	13
21	0	0	0	0	0	0	0	0	0	0	0	2	2
20	0	0	0	0	0	0	0	0	0	0	0	1	2
19	0	0	0	0	0	0	0	0	0	0	1	1	2
18	0	0	0	0	0	0	0	0	0	1	1	1	2
17	0	0	0	0	0	0	0	0	1	1	1	1	2
16	0	0	0	0	0	0	0	1	1	1	1	1	2
15	0	0	0	0	0	0	0	1	1	1	1	1	2
14	0	0	0	0	0	0	0	1	1	1	1	1	2
13	0	0	0	0	0	0	0	1	1	1	1	1	2
12	0	0	0	0	0	0	0	1	1	1	1	1	2
11	0	0	0	0	0	0	0	1	1	1	1	1	2
10	0	0	0	0	0	0	0	1	1	1	1	1	2
9	0	0	0	0	0	0	0	1	1	1	1	1	2
8	0	0	0	0	0	0	0	1	1	1	1	1	2
7	0	0	0	0	0	0	0	1	1	1	1	1	2
6	0	0	0	0	0	0	0	1	1	1	1	1	2
5	0	0	0	0	0	0	0	1	1	1	1	1	2
4	0	0	0	0	0	0	0	1	1	1	1	1	2
3	0	0	0	0	0	0	0	0	0	1	1	1	2
2	0	0	0	0	0	0	0	0	0	1	1	1	2
1	0	0	0	0	0	0	0	0	0	2	2	2	2

STRATO 2

0 CELLE SOLIDE
1 CELLE DI FLUIDO
2 CELLE DI CONTORNO APERTO

	1	2	3	4	5	6	7	8	9	10	11	12	13
21	0	0	0	0	0	0	0	2	2	2	2	2	2
20	0	0	0	0	0	0	0	1	1	1	1	1	2
19	0	0	0	0	0	0	1	1	1	1	1	1	2
18	0	0	0	0	0	1	1	1	1	1	1	1	2
17	0	0	0	0	1	1	1	1	1	1	1	1	2
16	0	0	0	0	1	1	1	1	1	1	1	1	2
15	0	0	0	0	1	1	1	1	1	1	1	1	2
14	0	0	0	0	1	1	1	1	1	1	1	1	2
13	0	0	0	0	1	1	1	1	1	1	1	1	2
12	0	0	0	0	1	1	1	1	1	1	1	1	2
11	0	0	0	0	1	1	1	1	1	1	1	1	2
10	0	0	0	0	1	1	1	1	1	1	1	1	2
9	0	0	0	0	1	1	1	1	1	1	1	1	2
8	0	0	0	0	1	1	1	1	1	1	1	1	2
7	0	0	0	0	1	1	1	1	1	1	1	1	2
6	0	0	0	0	1	1	1	1	1	1	1	1	2
5	0	0	0	0	1	1	1	1	1	1	1	1	2
4	0	0	0	0	1	1	1	1	1	1	1	1	2
3	0	0	0	0	0	1	1	1	1	1	1	1	2
2	0	0	0	0	0	0	0	1	1	1	1	1	2
1	0	0	0	0	0	0	0	2	2	2	2	2	2

Figure 4. Vado ligure topology for layers 1 (bottom) and 2.

STRATO 3

0 CELLE SOLIDE
1 CELLE DI FLUIDO
2 CELLE DI CONTORNO APERTO

	1	2	3	4	5	6	7	8	9	10	11	12	13
21	0	0	0	0	0	0	2	2	2	2	2	2	2
20	0	0	0	0	0	0	1	1	1	1	1	1	2
19	0	0	0	0	0	1	1	1	1	1	1	1	2
18	0	0	0	0	1	1	1	1	1	1	1	1	2
17	0	0	0	0	1	1	1	1	1	1	1	1	2
16	0	0	0	1	1	1	1	1	1	1	1	1	2
15	0	0	0	1	1	1	1	1	1	1	1	1	2
14	0	0	0	1	1	1	1	1	1	1	1	1	2
13	0	0	0	1	1	1	1	1	1	1	1	1	2
12	0	0	0	1	1	1	1	1	1	1	1	1	2
11	0	0	0	1	1	1	1	1	1	1	1	1	2
10	0	0	0	1	1	1	1	1	1	1	1	1	2
9	0	0	0	1	1	1	1	1	1	1	1	1	2
8	0	0	0	1	1	1	1	1	1	1	1	1	2
7	0	0	0	1	1	1	1	1	1	1	1	1	2
6	0	0	0	1	1	1	1	1	1	1	1	1	2
5	0	0	0	1	1	1	1	1	1	1	1	1	2
4	0	0	0	0	1	1	1	1	1	1	1	1	2
3	0	0	0	0	1	1	1	1	1	1	1	1	2
2	0	0	0	0	0	0	0	1	1	1	1	1	2
1	0	0	0	0	0	0	0	2	2	2	2	2	2

STRATO 4

0 CELLE SOLIDE
1 CELLE DI FLUIDO
2 CELLE DI CONTORNO APERTO

	1	2	3	4	5	6	7	8	9	10	11	12	13
21	0	0	0	0	0	0	2	2	2	2	2	2	2
20	0	0	0	0	0	0	1	1	1	1	1	1	2
19	0	0	0	0	1	1	1	1	1	1	1	1	2
18	0	0	0	0	1	1	1	1	1	1	1	1	2
17	0	0	1	1	1	1	1	1	1	1	1	1	2
16	0	0	1	1	1	1	1	1	1	1	1	1	2
15	0	1	1	1	1	1	1	1	1	1	1	1	2
14	0	1	1	1	1	1	1	1	1	1	1	1	2
13	0	1	1	1	1	1	1	1	1	1	1	1	2
12	0	1	1	1	1	1	1	1	1	1	1	1	2
11	0	1	1	1	1	1	1	1	1	1	1	1	2
10	0	1	1	1	1	1	1	1	1	1	1	1	2
9	0	1	1	1	1	1	1	1	1	1	1	1	2
8	0	1	1	1	1	1	1	1	1	1	1	1	2
7	0	1	1	1	1	1	1	1	1	1	1	1	2
6	0	1	1	1	1	1	1	1	1	1	1	1	2
5	0	1	1	1	1	1	1	1	1	1	1	1	2
4	0	1	1	1	1	1	1	1	1	1	1	1	2
3	0	0	1	1	1	1	1	1	1	1	1	1	2
2	0	0	0	0	1	1	0	1	1	1	1	1	2
1	0	0	0	0	0	0	0	2	2	2	2	2	2

Figure 5. Vado ligure topology for layers 3 and 4.

STRATO 5

0 CELLE SOLIDE
1 CELLE DI FLUIDO
2 CELLE DI CONTORNO APERTO

	1	2	3	4	5	6	7	8	9	10	11	12	13
21	0	0	0	0	0	0	2	2	2	2	2	2	2
20	0	0	0	0	0	0	1	1	1	1	1	1	2
19	0	0	0	0	1	1	1	1	1	1	1	1	2
18	0	0	0	0	1	1	1	1	1	1	1	1	2
17	0	0	1	1	1	1	1	1	1	1	1	1	2
16	0	0	1	1	1	1	1	1	1	1	1	1	2
15	0	1	1	1	1	1	1	1	1	1	1	1	2
14	0	1	1	1	1	1	1	1	1	1	1	1	2
13	0	1	1	1	1	1	1	1	1	1	1	1	2
12	0	1	1	1	1	1	1	1	1	1	1	1	2
11	0	1	1	1	1	1	1	1	1	1	1	1	2
10	2	1	1	1	1	1	1	1	1	1	1	1	2
9	2	1	1	1	1	1	1	1	1	1	1	1	2
8	0	1	1	1	1	1	1	1	1	1	1	1	2
7	0	1	1	1	1	1	1	1	1	1	1	1	2
6	0	1	1	1	1	1	1	1	1	1	1	1	2
5	0	1	1	1	1	1	1	1	1	1	1	1	2
4	0	1	1	1	1	1	1	1	1	1	1	1	2
3	0	0	1	1	1	1	1	1	1	1	1	1	2
2	0	0	0	0	1	1	0	1	1	1	1	1	2
1	0	0	0	0	0	0	0	2	2	2	2	2	2

STRATO 6

0 CELLE SOLIDE
1 CELLE DI FLUIDO
2 CELLE DI CONTORNO APERTO

	1	2	3	4	5	6	7	8	9	10	11	12	13
21	0	0	0	0	0	0	2	2	2	2	2	2	2
20	0	0	0	0	0	0	1	1	1	1	1	1	2
19	0	0	0	0	1	1	1	1	1	1	1	1	2
18	0	0	0	0	1	1	1	1	1	1	1	1	2
17	0	0	1	1	1	1	1	1	1	1	1	1	2
16	0	0	1	1	1	1	1	1	1	1	1	1	2
15	0	1	1	1	1	1	1	1	1	1	1	1	2
14	0	1	1	1	1	1	1	1	1	1	1	1	2
13	0	1	1	1	1	1	1	1	1	1	1	1	2
12	0	1	1	1	1	1	1	1	1	1	1	1	2
11	0	1	1	1	1	1	1	1	1	1	1	1	2
10	2	1	1	1	1	1	1	1	1	1	1	1	2
9	2	1	1	1	1	1	1	1	1	1	1	1	2
8	0	1	1	1	1	1	1	1	1	1	1	1	2
7	0	1	1	1	1	1	1	1	1	1	1	1	2
6	0	1	1	1	1	1	1	1	1	1	1	1	2
5	0	1	1	1	1	1	1	1	1	1	1	1	2
4	0	1	1	1	1	1	1	1	1	1	1	1	2
3	0	0	1	1	1	1	1	1	1	1	1	1	2
2	0	0	0	0	1	1	0	1	1	1	1	1	2
1	0	0	0	0	0	0	0	2	2	2	2	2	2

Figure 6. Vado ligure topology for layers 5 and 6 (surface); cells (9.1) and (10.1) represent the discharge channel.